Final Report – DE-FG03-99ER45791

PIs: Ellen R. Fisher and Peter K. Dorhout
Department of Chemistry, Colorado State University

At the end of the funding period (March 2003) for our program in ferroelectric oxide nanomaterials, we had 3 publications in print,[1-3] one more had been submitted[4] and two more were in preparation,[5,6] in peer-reviewed journals and 6 invited symposia lectures had been given since starting the project in the Fall of 1999. We hired two postdoctoral fellows, Dr. Ki-Seog Chang and Dr. Wenzhong Wang. We have also trained two graduate students, Ms. Keri Williams and Ms. Bernadette Hernandez, and one undergraduate student (Mr. Michael Scancella).

Below is an outline of our specific aims and the goals we obtained during the funding period.

Year 1

The team prepared and analyzed samples of nanocrystalline materials prepared by three complementary synthetic schemes:

- Plasma deposition
- Melt deposition
- Sol-gel deposition

Plasma deposition comprises an argon plasma that etches pre-formed buttons or powders of target precursors to affect vaporization and subsequent deposition within porous aluminum oxide templates. As outlined in the original proposal, the templates comprised a set of monodisperse pores of variable diameter (10 - 200 nm) and significant depth (30 - 50 microns). By selecting appropriate templates, rods or hollow cylinders of material can be created whose aspect ratios are enormous.

Initial attempts at plasma deposition of bismuth telluride precursors resulted in the vaporization of target material but with uncontrolled deposition - black material was found on most surfaces of the reactor. Initial electron microscope imaging did not show significant deposition of material within the template. Grazing-angle X-ray diffraction studies also confirmed that little material was isolated within the template pores.

For the remainder of the first and second years, the aims of using plasma deposition for the project did not deviate from our initial focus. Optimization of the plasma deposition parameters was performed by adjusting the plasma power and carrier gas composition as well as precursor selection. We also modified a plasma reactor to incorporate solution injections that would rely less on target compound "sputtering" and more on solution volatilization to create a reactive plasma that enabled suitable product deposition.

Melt deposition of target precursors also provided mixed results. It was necessary to develop a low-melting eutectic material that would not react with our template material at

moderate temperatures. We selected antimony sulfide, Sb_2S_3, as a suitable solvent for our precursors. A variety of ternary and quaternary systems were evaluated for the following traits:

a) moderate melting temperatures : 400 – 700 °C
b) minimal reactivity with alumina
c) complex phase formation and/or congruent melting characteristics

A set of material compositions were evaluated by thermal analysis and $Ag_2Sb_2S_4/Sb_2S_3$ was selected for initial trials as this mixture melts at 560 °C. Black templates emerged from our melt-dipping process. These solids were evaluated for their crystallinity and chemical composition but little or no rodlike materials resulted.

The sol-gel deposition of materials displayed some of the most promising results for nanotube and nanorod formation. Sol-gels of $BaTiO_3$ and $SrTiO_3$ ferroelectric precursors were prepared from titanium isopropoxide and alkaline-earth metal acetate salts according to literature precedence. Ms. Hernandez traveled to Sandia Laboratory to learn sol-gel processing techniques in 2000. Various trials to prepare gels of different viscosities were attempted and gelation was controlled by the use of humidity chambers. The gel-impregnated templates were fired at sintering temperatures of 600 °C to affect monolith formation within the templates. Templates with pores of 200 nm and 50 nm were used for the initial studies.

Year 2

Electron microscopy showed that we were able to fill the pores of the membranes with our target oxide materials. Shown in Fig. 2, below, are the nanoscopic tubules of $BaTiO_3$. Microanalysis of the structures by EDS showed emission lines for titanium and barium. Based on the analysis of this figure, we determined that tubules rather than rods formed from this reaction. Rods may be formed by changing the concentration of the gel or the template.

The image in Fig. 2a demonstrates that high-aspect ratio material was prepared, and grazing-angle incidence X-ray diffraction studies (Fig. 2b) confirm that crystalline $BaTiO_3$ material was formed in the templates. Raman spectroscopy also confirmed the presence of the perovskite phase. We made dielectric constant measurements of our tubules and rods to search for the phase change associated with the tratragonal to cubic (non-ferroelectric) transition at 120 °C. Thermal analysis (DSC) plots and dielectric measurements of the materials have shown us that the nanoparticles of $BaTiO_3$ were mostly in the cubic (non-ferroelectric) phase. We were able to modify our process time and temperatures to prepare only the tetragonal (ferroelectric) phase. In addition to the ferroelectric barium titanate, the ferroelectric phase of $PbTiO_3$ has been prepared by our group and we are currently working on methods (see below) to prepare solid-solutions of Sr/Pb materials (with a lower T_c than $PbTiO_3$ (T_c = 200 °C)).

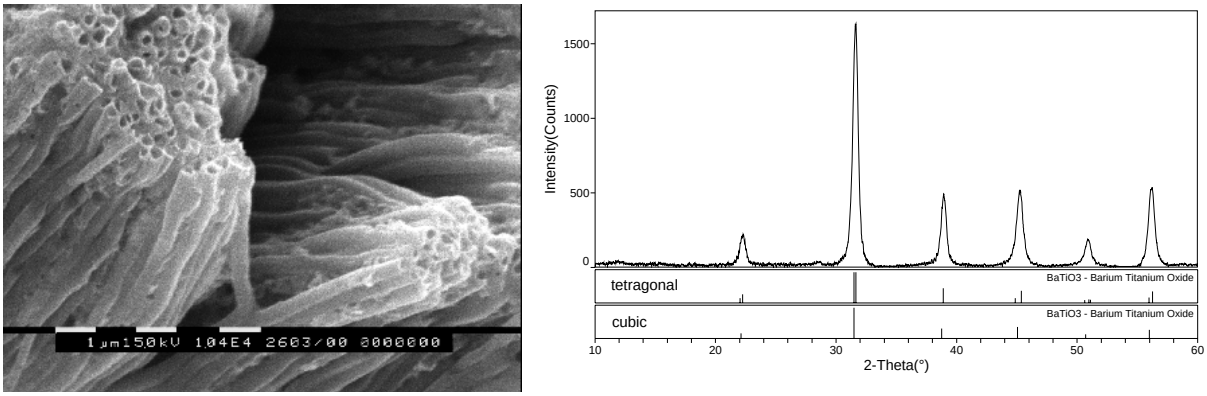

(a) (b)

Fig. 2. (a) SEM image of $BaTiO_3$-nanotubes removed from the template showing the hollow nature of the tubes. (b) Powder X-ray diffraction pattern for bulk samples calcined from 700°C to 900°C were the same. Diffraction peaks match up with tetragonal phase.

Finally, transmission electron micrographs enabled us to evaluate the materials formed in the porous membranes. Isolated rods of $BaTiO_3$ were evaluated and found to be the cubic phase. A TEM micrograph is shown in Fig. 3a, along with the electron diffraction image from those rods, Fig. 3b. White crystallites of NaOH (used to dissolve the alumina template) have grown on the nanorods of $BaTiO_3$. Imaging of all samples provides relative crystallinity and crystal growth directions.

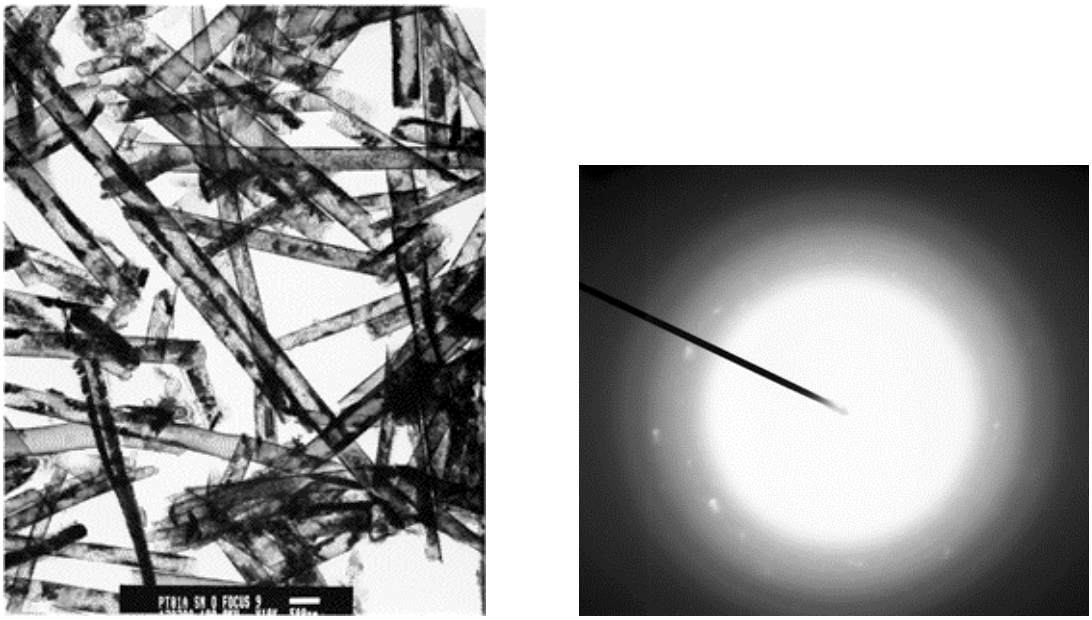

(a) (b)

Fig. 3. (a) TEM image of nanotubes of $BaTiO_3$ prepared at 700 °C, and the resulting electron diffraction image (b). Some degree of single crystal growth can be seen but this image indicates that the crystallites are small (~ 5 nm) and non-directional in growth.

Year 3.

During Year 3 of the grant, phosphates were synthesized by a sol-gel deposition into porous alumina templates. After firing at a variety of different temperatures, the phase and luminescent properties were investigated. For example, Eu doped (5 mol %) $LaPO_4$ was prepared by sol-gel deposition in porous alumina anodic membranes. After sintered at 650ºC for 3 h, the membranes were removed. SEM images revealed that the as-prepared phosphate retains its tubular structure, Fig. 4A. EDS showed the characteristic lines of La and P and XRD confirmed the structure to be the phosphate. The diameter of the tubes was around 200 nm, the pore size of the template membranes. Fluorescence spectra of the phosphate nanotubes demonstrated strong emission peaks that are characteristic of Eu emission, Fig. 4B.[7-9] The morphology of the phosphate nanotubes could be changed by the concentration of the sol or deposition parameter. The size of the nanotubes may be changed based on the template employed.

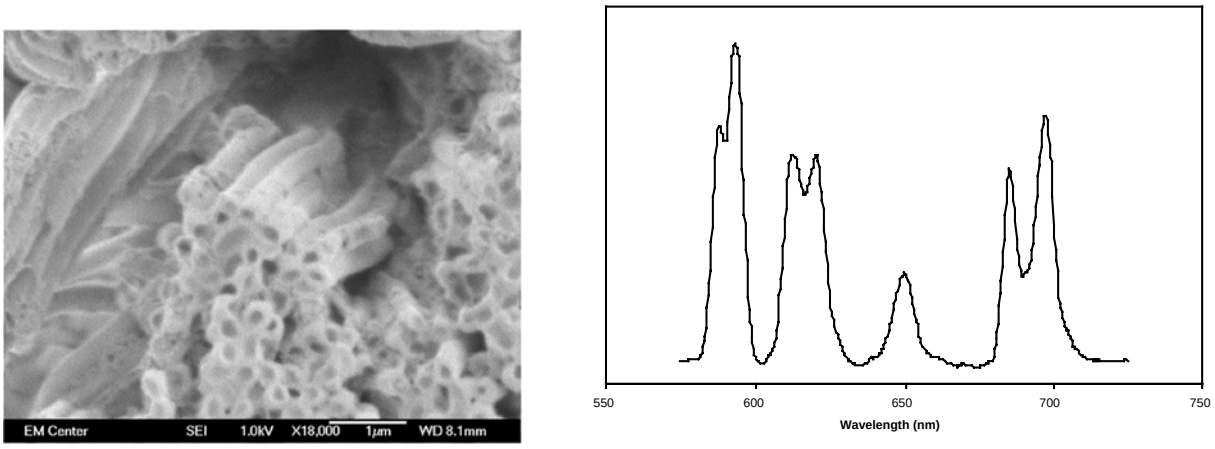

(a) *(b)*

Fig. 4 (a) Free-standing nanotubes of Eu:$LaPO_4$ formed in an alumina matrix and (b) the room-temperature luminescence spectrum (intensity vs. wavelength, nm) from the 5% Eu doped nanotubes.

Subsequent to the funding period of the grant, we have completed a number of the projects that began in the funding period. These include studies of the titanates (Ba, Sr, Pb) and $PbZrO_3$,[1,8,10] studies of the Eu-doped lanthanum phosphate nanotubes,[4,5] and new studies of $NdNiO_3$ and O_3 nanotubes.

References

(1) Hernandez, B. A.; Chang, K.-S.; Fisher, E. R.; Dorhout, P. K. *Chem. Mater.* "Examination of Size-Induced Ferroelectric Phase Transitions in Template Synthesized $PbTiO_3$ Nanotubes and Nanofibers" **2004**, in press.

(2) Hernandez, B. A.; Chang, K.-S.; Fisher, E. R.; Dorhout, P. K. *Chem. Mater.* "Sol-gel template synthesis and characterization of $BaTiO_3$ and $PbTiO_3$ nanotubes" **2002**, *14*, 480-482.

(3) Chang, K.-S.; Hernandez, B. A.; Fisher, E. R.; Dorhout, P. K. *J. Korean. Chem. Soc.* "Sol-gel template synthesis and characterization of PT, PZ, and PZT nanotubes" **2002**, *46*, 242-251.

(4) Wang, W.; Fisher, E. R.; Dorhout, P. K. *Chem. Mater.* "Rare-earth ion-doped Lanthanum Phosphate Nanotubes Prepared by Template Synthesis" **2004**, submitted.

(5) Wang, W.; Fisher, E. R.; Dorhout, P. K. *Nanotech.* "Preparation of Nanostructured $LaPO_4$:(Ce,Tb) Phosphors" **2004**, in preparation.

(6) Hernandez, B. A.; Fisher, E. R.; Dorhout, P. K. *Nanotech.* "Preparation of $NbNiO_3$ Nanostructures" **2004**, in preparation.

(7) Williams, D. K.; Yuan, H.; Tissue, B. M. *Journal of Luminescence* "Size dependence of the luminescence spectra and dynamics of Eu^{3+}: Y_2O_3 nanocrystals" **1999**, *83-4*, 297-300.

(8) Meltzer, R. S.; Feofilov, S. P.; Tissue, B.; Yuan, H. B. *Phys. Rev. B* "Dependence of fluorescence lifetimes of Eu^{3+}: Y_2O_3 nanoparticles on the surrounding medium" **1999**, *60*, R14012-R14015.

(9) Williams, D. K.; Bihari, B.; Tissue, B. M.; McHale, J. M. *J. Phys. Chem. B* "Preparation and fluorescence spectroscopy of bulk monoclinic Eu^{3+}: Y_2O_3 and comparison Eu^{3+}: Y_2O_3 nanocrystals" **1998**, *102*, 916-920.

(10) Hernandez-Sanchez, B. A. "Template Synthesis of One-Dimensional Perovskites (ABO_3): An Investigation of the Effects of Grain Size and Aspect Ratio on the Electronic Properties" Ph. D. Thesis, Colorado State University,153 pp.